Models and Raman Analysis of Molecular Nanofilms Conjugated on Photonic Crystal Slabs

Zheng Wang[a, b], Chao Liu[a], Erwen Li[c], Swapnajit Chakravarty[d], Alan X. Wang*[, c], D.L. Fan*[, a, e], and Ray T. Chen* [,a,b,d]

[a]Materials Science and Engineering Program, Texas Materials Institute, The University of Texas at Austin, Austin, TX USA 78712;
[b]Dept. of Electrical and Computer Engineering, The University of Texas at Austin, 10100 Burnet Rd., MER 160, Austin, TX USA 78758;
[c]School of Electrical Engineering and Computer Science, Oregon State University, Corvallis, OR, 97331, USA;
[d]Omega Optics, Inc., 8500 Shoal Creek Blvd., Bldg. 4, Suite 200, Austin, TX USA 78757;
[e]Dept. of Mechanical Engineering, the University of Texas at Austin, Austin, TX USA 78712;

ABSTRACT

Photonic crystal slabs (PCSs), which generally consist of two-dimensional arrays of nanoholes in the top layer of a dual layer dielectric film, have been demonstrated as a promising platform for optical biosensing. Both the Fano resonance in a perfect PCS and the Lorentzian resonance in a micro-cavity resulted from an introduced defect in PCS have been studied. While, the use of resonance peak shift for detecting molecules owing to the change of the refractive index is a nonspecific biosensing technique. Biorecognition molecules, such as antibodies that can specific bond to interesting molecules, are conjugated on the PCS to improve the detection specificity. It is a widely adopted assumption that the conjugated molecules form into a uniform nanofilm in the PCS based biosensors, which covers either the entire surface of the dielectric layer or the entire sidewalls of nanoholes. However, the actual device performance is much lower than that obtained based on this assumption, which suggests the over-simplicity of the hypothesis above. It is of keen interest to reveal the actual arrangement and distribution of molecules on PCS for designing high-performance PCS biosensors. Here, we propose models and analysis of the distribution of nanofilms on PCS. We employed Raman scattering technique to experimentally reveal the actual various configurations of nanofilms, which support our theoretical modeling. The results obtained in this research can be essential for designing high-performance PCS based nanobiosensors.

Keywords: Surface-Enhanced Raman Scattering, Photonic Crystal, Guided-Mode Resonance

1. INTRODUCTION

Photonic crystals (PCs), which are periodic structures with a high and low refractive index contrast modulation, have recently become highly desirable platforms for manipulation of light [1]. One could design the periodic nanostructures to form photonic band-gaps, within which the propagation of light is forbidden. Since it remains challenging to fabricate three-dimensional structures with COMS compatible approaches, we employ the use of two-dimensional PC that photonic crystal slabs (PCS) instead, with which we still achieve essential photonic band gaps and future engineer the band-gaps for specific applications[2-8]. Among all applications, building ultra-sensitive sensors for biological, medical, and military proposes have been attracting tremendous interests. Both the Fano resonance in a perfect PCS [9-12] and the Lorentzian resonance in a micro-cavity resulted from an introduced defect in PCS [13-18] have been studied intensively. While the use of resonance peak shift for detecting molecules owing to the change of the refractive index is a nonspecific biosensing technique. Biorecognition molecules, such as antibodies that can specific bond to interesting molecules, have

* wang@eecs.oregonstate.edu; dfan@austin.utexas.edu; chenrt@austin.utexas.edu

Nanoscale Imaging, Sensing, and Actuation for Biomedical Applications XIV, edited by Alexander N. Cartwright, Dan V. Nicolau, Proc. of SPIE Vol. 10077, 100770G
© 2017 SPIE · CCC code: 1605-7422/17/$18 · doi: 10.1117/12.2253392

to be conjugated on the PCS to improve the detection specificity [19-22]. It is a widely adopted assumption that the conjugated molecules form into a uniform nanofilm in the PCS based biosensors, which covers either the entire surface of the dielectric layer or the entire sidewalls of nanoholes. However, the actual device performance is much lower than that obtained based on this assumption, which suggests the over-simplicity of the assumption above. It is of great interest to reveal the actual arrangement and distribution of molecules on PCSs for designing high-performance PCS based biosensors. Here, we propose models and analysis of the distribution of nanofilms on PCS. We employed Raman scattering technique to experimentally reveal the actual various configurations of nanofilms. For the different design of PCSs, the electromagnetic field distribution will change, and the model overlap with conjugated nanofilms will be different. The $|\mathbf{E}|^4$ enhancement dependency of Raman scattering would magnify the deviation of the configurations of nanofilms. One could compare the numerically simulated enhancement with experimental observations to achieve the necessary information about the configuration of nanofilms.

2. FABRICATION AND RAMAN MEASUREMENT

We fabricated PCSs with CMOS compatible process. The fabrication flow of PCSs is illustrated in Fig. 1. In brief, the fabrication starts with creating a two-dimensional ordered array of nanoholes on a 230 nm thick Si_3N_4 film, which is deposited on a fused silica substrate, via EBL followed by reactive ion etching (RIE). The conductive polymer is used to reduce charging effects because the substrate is insulating. For future CMOS-compatible manufacturing with DUV lithography, this issue could be safely ignored.

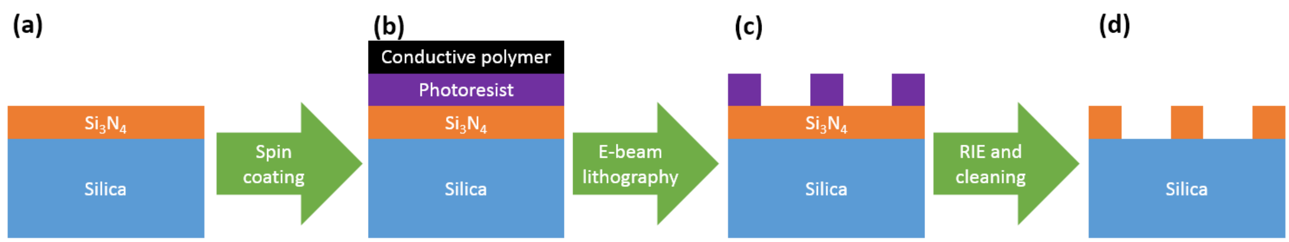

Fig. 1. Fabrication flow of PCSs

Figure 2a shows a typical scanning electron microscopy (SEM) image of a fabricated PCS. In experiments, we measured the Raman signal of 1 mM Nile blue solution dried on PCSs and focused on the 597 cm^{-1} Raman mode. Figure 2b shows typical Raman spectra of 1 mM Nile blue around the 597 cm^{-1} mode. To ensure the rigidity of measurements, for each design (include the reference one), we randomly select at least 5 points to measure the intensity of Raman signals, which is shown in Fig. 2c.

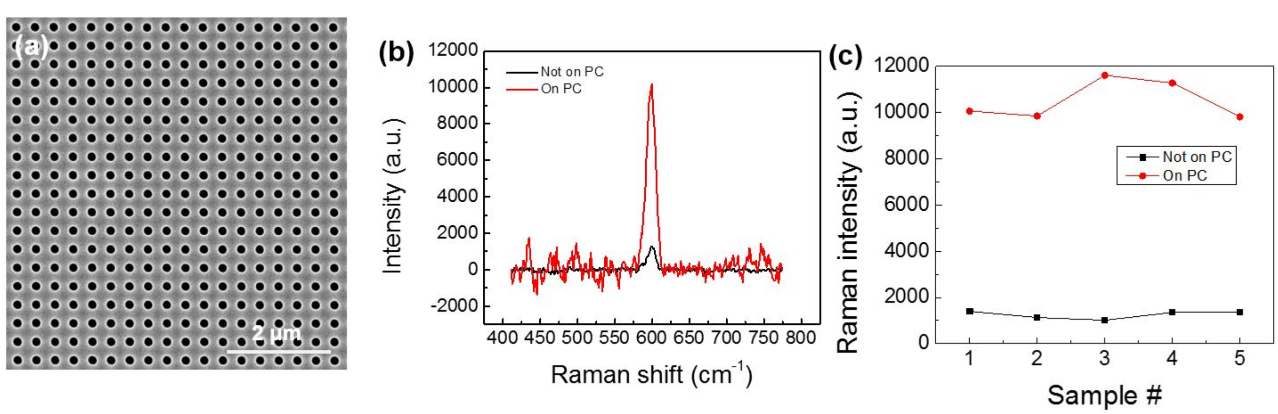

Fig. 2. (a) Typical SEM image of a PCS. (b) Typical Raman spectra of 1 mM Nile blue. (c) Raman intensity of multiple measurements.

3. NUMERICAL SIMULATION AND MODELING

We simulate the electromagnetic field distribution of PCSs via Stanford stratified structure solver (S^4), which is a frequency domain linear Maxwell's equations solver for layered periodic structures [23]. The rigorous coupled-wave analysis (RCWA) algorithm enables S4 to be a fast, precise, and effective approach with numerous experimental demonstrations in multiple research areas [24-35]. We exam two extreme scenarios of configurations of nanofilms: "fully anisotropic" (FA) and "uniform nanofilm" (UN), shown in Fig. 3(a) and (b), respectively. For the FA case, there would be no molecules attached to the side wall of the nanoholes of PCSs. While in UN case, there would be a nanofilm of molecules, which cover the surface of PCS including the sidewall with the same thickness everywhere. We simulated the electromagnetic field distribution of 3 different designs of PCSs. A typical simulated distribution of electromagnetic field is shown in Fig. 3(c). With the distribution of electromagnetic field, we calculated the enhancements of Raman scattering and summarized in Table 1. The enhancements of Raman scattering measured from experiments are also listed in Table 1 for comparison.

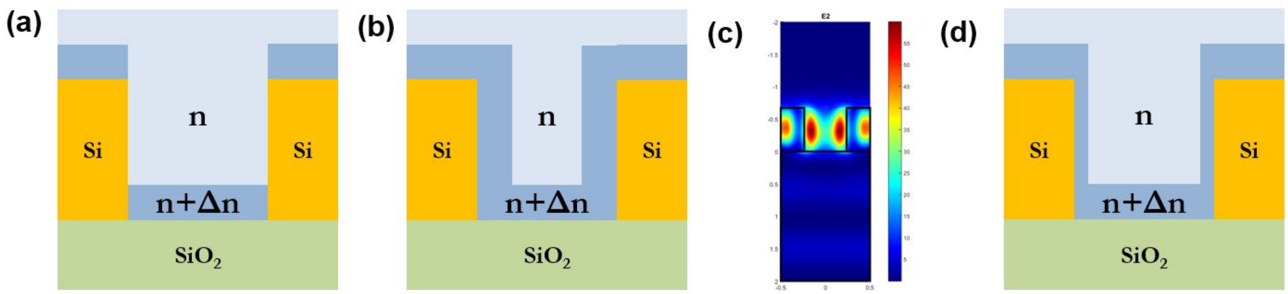

Fig. 3. (a) Schematic of "fully anisotropic" configuration. (b) Schematic of "uniform nanofilm" configuration (c) Typical simulated distribution of electromagnetic field via S^4. (d) Schematic of the more realistic configuration.

Table 1. Enhancements of Raman scattering from simulations and experiments

	FA configuration	UN configuration	Experiment
Design 1	0.81	5.8	4.34 ± 1.28
Design 2	1.21	18.7	8.42 ± 1.33
Design 3	4.45	48.12	13.56 ± 1.87

4. DISCUSSION AND CONCLUSION

By comparing the simulated results and experimental observations, one could find out a more realistic configuration of nanofilms on PCSs should be an ununiformed cover, which is illustrated in Fig. 3(d). There are molecules on the sidewalls of nanoholes which constituted the PCSs, while with a thinner thickness. In conclusion, we employed Raman scattering technique to experimentally reveal the configurations of nanofilms, which support our theoretical modeling. The results suggest that the widely adopted assumption that the conjugated molecules form into a uniform nanofilm in the PCS based biosensors which covers either the entire surface of the dielectric layer or the entire sidewalls of nanoholes is over-simplicity. A more realistic configuration of nanofilm should be uniformed and the thickness of the nanofilm on the sidewalls of nanoholes are thinner. The results obtained in this research can be essential for designing high-performance PCS based nanobiosensors.

ACKNOWLEDGEMENT

The authors are grateful for the support of National Institutes of Health (NIH) (Grant No. 9R42ES024023-02 and 5R42ES024023-03) and Welch Foundation (Grant No. F-1734).

REFERENCES

[1] D. J. Norris, “Photonic Crystals: A view of the future,” Nature materials, 6(3), 177-178 (2007).
[2] E. Chow, S. Lin, S. Johnson *et al.*, “Three-dimensional control of light in a two-dimensional photonic crystal slab,” Nature, 407(6807), 983-986 (2000).
[3] M. S. Kushwaha, and B. Djafari-Rouhani, “Band-gap engineering in two-dimensional periodic photonic crystals,” Journal of Applied Physics, 88(5), 2877-2884 (2000).
[4] S. Kubo, D. Mori, and T. Baba, “Low-group-velocity and low-dispersion slow light in photonic crystal waveguides,” Optics Letters, 32(20), 2981-2983 (2007).
[5] T. Baba, “Slow light in photonic crystals,” Nature Photonics, 2(8), 465-473 (2008).
[6] T. P. White, L. C. Botten, C. M. de Sterke *et al.*, “Efficient slow-light coupling in a photonic crystal waveguide without transition region,” Optics Letters, 33(22), 2644-2646 (2008).
[7] S. G. Yang, H. W. Chen, C. Y. Qiu *et al.*, “Slow-light delay enhancement in small-core pure silica photonic crystal fiber based on Brillouin scattering,” Optics Letters, 33(2), 95-97 (2008).
[8] D. Schneider, F. Liaqat, E. H. El Boudouti *et al.*, “Engineering the Hypersonic Phononic Band Gap of Hybrid Bragg Stacks,” Nano Letters, 12(6), 3101-3108 (2012).
[9] N. Ganesh, W. Zhang, P. C. Mathias *et al.*, “Enhanced fluorescence emission from quantum dots on a photonic crystal surface,” Nature Nanotechnology, 2(8), 515-520 (2007).
[10] N. Ganesh, I. D. Block, P. C. Mathias *et al.*, “Leaky-mode assisted fluorescence extraction: application to fluorescence enhancement biosensors,” Optics Express, 16(26), 21626-21640 (2008).
[11] M. Huang, A. A. Yanik, T. Y. Chang *et al.*, “Sub-wavelength nanofluidics in photonic crystal sensors,” Optics Express, 17(26), 24224-24233 (2009).
[12] Y. J. Huang, G. Pandraud, and P. M. Sarro, “Reflectance-based two-dimensional TiO2 photonic crystal liquid sensors,” Optics Letters, 37(15), 3162-3164 (2012).
[13] W. C. Lai, S. Chakravarty, Y. Zou *et al.*, “Silicon nano-membrane based photonic crystal microcavities for high sensitivity bio-sensing,” Optics Letters, 37(7), 1208-1210 (2012).
[14] Y. Zou, S. Chakravarty, W. C. Lai *et al.*, “Methods to array photonic crystal microcavities for high throughput high sensitivity biosensing on a silicon-chip based platform,” Lab on a Chip, 12(13), 2309-2312 (2012).
[15] S. R. Hu, Y. L. Zhao, K. Qin *et al.*, “Enhancing the Sensitivity of Label-Free Silicon Photonic Biosensors through Increased Probe Molecule Density,” Acs Photonics, 1(7), 590-597 (2014).
[16] D. Q. Yang, S. Kita, F. Liang *et al.*, “High sensitivity and high Q-factor nanoslotted parallel quadrabeam photonic crystal cavity for real-time and label-free sensing,” Applied Physics Letters, 105(6), (2014).
[17] Z. Wang, H. Yan, S. Chakravarty *et al.*, “Microfluidic channels with ultralow-loss waveguide crossings for various chip-integrated photonic sensors,” Optics Letters, 40(7), 1563-1566 (2015).
[18] H. Yan, Y. Zou, S. Chakravarty *et al.*, “Silicon on-chip bandpass filters for the multiplexing of high sensitivity photonic crystal microcavity biosensors,” Applied Physics Letters, 106(12), (2015).
[19] M. C. Estevez, M. Alvarez, and L. M. Lechuga, “Integrated optical devices for lab-on-a-chip biosensing applications,” Laser & Photonics Reviews, 6(4), 463-487 (2012).
[20] J. Yang, F. Ren, X. Chong *et al.*, "Guided-Mode Resonance Grating with Self-Assembled Silver Nanoparticles for Surface-Enhanced Raman Scattering Spectroscopy." 1, 380-389.
[21] Y. N. Zhang, Y. Zhao, and R. Q. Lv, “A review for optical sensors based on photonic crystal cavities,” Sensors and Actuators a-Physical, 233, 374-389 (2015).
[22] A. F. Gavela, D. G. Garcia, J. C. Ramirez *et al.*, “Last Advances in Silicon-Based Optical Biosensors,” Sensors, 16(3), (2016).
[23] V. Liu, and S. H. Fan, “S-4: A free electromagnetic solver for layered periodic structures,” Computer Physics Communications, 183(10), 2233-2244 (2012).

[24]O. Kilic, S. Kim, W. Suh *et al.*, "Photonic crystal slabs demonstrating strong broadband suppression of transmission in the presence of disorders," Optics Letters, 29(23), 2782-2784 (2004).
[25]Y. C. Shuai, D. Y. Zhao, A. S. Chadha *et al.*, "Coupled double-layer Fano resonance photonic crystal filters with lattice-displacement," Applied Physics Letters, 103(24), (2013).
[26]Y. C. Shuai, D. Y. Zhao, Z. B. Tian *et al.*, "Double-layer Fano resonance photonic crystal filters," Optics Express, 21(21), 24582-24589 (2013).
[27]Y. H. Liu, A. Chadha, D. Y. Zhao *et al.*, "Approaching total absorption at near infrared in a large area monolayer graphene by critical coupling," Applied Physics Letters, 105(18), (2014).
[28]D. Zhao, H. Yang, J.-H. Seo *et al.*, "Design and Characterization of Photonic Crystal Membrane Reflector Based Vertical Cavity Surface Emitting Lasers on Silicon," Reviews in Nanoscience and Nanotechnology, 3(2), 77-87 (2014).
[29]R. Gad, W. T. Lau, C. Nicholaou *et al.*, "Tailoring of spectral response and spatial field distribution with corrugated photonic crystal slab," Optics Letters, 40(16), 3715-3718 (2015).
[30]V. K. Narasimhan, T. M. Hymel, R. A. Lai *et al.*, "Hybrid Metal–Semiconductor Nanostructure for Ultrahigh Optical Absorption and Low Electrical Resistance at Optoelectronic Interfaces," ACS Nano, 9(11), 10590-10597 (2015).
[31]Y. L. Xu, T. Gong, and J. N. Munday, "The generalized Shockley-Queisser limit for nanostructured solar cells," Scientific Reports, 5, (2015).
[32]J. R. Piper, and S. H. Fan, "Broadband Absorption Enhancement in Solar Cells with an Atomically Thin Active Layer," Acs Photonics, 3(4), 571-577 (2016).
[33]E. C. Regan, Y. C. Shen, J. J. Lopez *et al.*, "Substrate-Independent Light Confinement in Bioinspired All Dielectric Surface Resonators," Acs Photonics, 3(4), 532-536 (2016).
[34]A. Yang, K. Yang, H. Yu *et al.*, "Piezoelectric tuning of narrowband perfect plasmonic absorbers via an optomechanic cavity," Optics Letters, 41(12), 2803-2806 (2016).
[35]C. Liu, Z. Wang, E. Li *et al.*, "Electrokinetic-Manipulation Integrated Plasmonic-Photonic Hybrid Raman Nanosensors with Dual Enhanced sensitivity," ACS Sensors, (2017).